Stanford Synchrotron Radiation Lightsource (SSRL) Beamline 12-2, the National Institute of General Medical Sciences and National Cancer Institute Structural Biology Facility (GM/CA) at the Advanced Photon Source (APS), and the Advanced Light Source (ALS) beamline 8.2.1 for support with x-ray diffraction measurements. We acknowledge the Gordon and Betty Moore Foundation, the Beckman Institute, and the Sanofi-Aventis Bioengineering Research Program for support of the Molecular Observatory at the California Institute of Technology (Caltech). The operations at the SSRL, ALS, and APS are supported by the U.S. Department of Energy and the NIH. GM/CA has been funded in whole or in part with federal funds from the National Cancer Institute (ACB-12002) and the National Institute of General Medical Sciences (AGM-12006). T.S. was supported by a Postdoctoral Fellowship of the Deutsche Forschungsgemeinschaft. S.P. and D.H.L are Amgen Graduate Fellows, supported through the Caltech-Amgen Research Collaboration. F.M.H. was supported by a Ph.D. student fellowship of the Boehringer Ingelheim Fonds. S.K. was supported by NIH Awards R01-GM090324 and U54-GM087519 and by the University of Chicago Comprehensive Cancer Center (P30-CA014599). A.A.K. was supported by NIH awards U01-GM094588 and U54-GM087519 and by Searle Funds at The Chicago Community Trust. A.H. was supported by Caltech startup funds, the Albert Wyrick V Scholar Award of the V Foundation for Cancer Research, the 54th Mallinckrodt Scholar Award of the Edward Mallinckrodt Jr. Foundation, a Kimmel Scholar Award of the Sidney Kimmel Foundation for Cancer Research, a Camille-Dreyfus Teacher Scholar Award of The Camille and Henry Dreyfus Foundation, and NIH grant R01-GM111461. The coordinates and structure factors have been deposited with the Protein Data Bank with accession codes 5CWV (Nup192^{TAIL}), 5CWU (Nup188^{TAIL}), 4JQ5 (*hs*Nup49$^{CCS2+3*}$), 4JNV and 4JNU (*hs*Nup57^{CCS3*}), 5CWT (Nup57^{CCS3*}), 4JO7 (*hs*Nup49$^{CCS2+3*}$•*hs*Nup57^{CCS3*}, 2:2 stoichiometry), 4JO9 (*hs*Nup49$^{CCS2+3*}$•*hs*Nup57^{CCS3*}, 1:2 stoichiometry), 5CWW (Nup82^{NTD}•Nup159^{T}•Nup145N^{APD}), and 5CWS (CNT•Nic96^{R1}•sAB-158). The authors declare no financial conflicts of interest. S.K. and A.K. are inventors on a patent application filed by the University of Chicago that covers a design of monobody libraries (US 13/813,409). Monobodies are available from S.K. under a material transfer agreement with the University of Chicago.

SUPPLEMENTARY MATERIALS

www.sciencemag.org/content/350/6256/56/suppl/DC1
Materials and Methods
Figs. S1 to S38
Tables S1 to S9
Movies S1 to S4
References (*42*–*65*)

29 June 2015; accepted 12 August 2015
Published online 27 August 2015
10.1126/science.aac9176

REPORTS

PLANETARY SCIENCE

Discovery and spectroscopy of the young jovian planet 51 Eri b with the Gemini Planet Imager

B. Macintosh,[1,2]* J. R. Graham,[3] T. Barman,[4] R. J. De Rosa,[3] Q. Konopacky,[5] M. S. Marley,[6] C. Marois,[7,8] E. L. Nielsen,[9,1] L. Pueyo,[10] A. Rajan,[11] J. Rameau,[12] D. Saumon,[13] J. J. Wang,[3] J. Patience,[11] M. Ammons,[2] P. Arriaga,[14] E. Artigau,[12] S. Beckwith,[3] J. Brewster,[9] S. Bruzzone,[15] J. Bulger,[11,16] B. Burningham,[6,17] A. S. Burrows,[18] C. Chen,[10] E. Chiang,[3] J. K. Chilcote,[19] R. I. Dawson,[3] R. Dong,[3] R. Doyon,[12] Z. H. Draper,[8,7] G. Duchêne,[3,20] T. M. Esposito,[14] D. Fabrycky,[21] M. P. Fitzgerald,[14] K. B. Follette,[1] J. J. Fortney,[22] B. Gerard,[8,7] S. Goodsell,[23,24] A. Z. Greenbaum,[25,10] P. Hibon,[24] S. Hinkley,[26] T. H. Cotten,[27] L.-W. Hung,[14] P. Ingraham,[28] M. Johnson-Groh,[8,7] P. Kalas,[3,9] D. Lafreniere,[12] J. E. Larkin,[14] J. Lee,[27] M. Line,[22] D. Long,[10] J. Maire,[19] F. Marchis,[9] B. C. Matthews,[7,8] C. E. Max,[22] S. Metchev,[15,29] M. A. Millar-Blanchaer,[30] T. Mittal,[3] C. V. Morley,[22] K. M. Morzinski,[31] R. Murray-Clay,[32] R. Oppenheimer,[33] D. W. Palmer,[2] R. Patel,[29] M. D. Perrin,[10] L. A. Poyneer,[2] R. R. Rafikov,[18] F. T. Rantakyrö,[24] E. L. Rice,[34,33] P. Rojo,[35] A. R. Rudy,[22] J.-B. Ruffio,[1,9] M. T. Ruiz,[35] N. Sadakuni,[36,24] L. Saddlemyer,[7] M. Salama,[3] D. Savransky,[37] A. C. Schneider,[38] A. Sivaramakrishnan,[10] I. Song,[27] R. Soummer,[10] S. Thomas,[28] G. Vasisht,[39] J. K. Wallace,[39] K. Ward-Duong,[11] S. J. Wiktorowicz,[22] S. G. Wolff,[25,10] B. Zuckerman[14]

Directly detecting thermal emission from young extrasolar planets allows measurement of their atmospheric compositions and luminosities, which are influenced by their formation mechanisms. Using the Gemini Planet Imager, we discovered a planet orbiting the ~20-million-year-old star 51 Eridani at a projected separation of 13 astronomical units. Near-infrared observations show a spectrum with strong methane and water-vapor absorption. Modeling of the spectra and photometry yields a luminosity (normalized by the luminosity of the Sun) of 1.6 to 4.0 × 10^{-6} and an effective temperature of 600 to 750 kelvin. For this age and luminosity, "hot-start" formation models indicate a mass twice that of Jupiter. This planet also has a sufficiently low luminosity to be consistent with the "cold-start" core-accretion process that may have formed Jupiter.

Several young, self-luminous extrasolar planets have been directly imaged at infrared (IR) wavelengths (*1*–*8*). The planets directly imaged to date are massive [(estimated at 5 to 13 Jupiter masses (M_J)] and positioned at large separations [9 to 650 astronomical units (AU)] from their host star, compared with planets in our solar system. Photometry and spectroscopy can be used to probe the atmospheres of these young jovian planets, providing clues about their formation. Several unexpected results have emerged. The near-IR colors of these planets are mostly red, indicating cloudy atmospheres similar to those of brown dwarfs of spectral type L. Methane absorption features are prominent in the near-IR spectra of T dwarfs [effective temperature (T_{eff}) < 1100 K], as well as in the giant planets of our solar system, but such features are weak or absent in the directly imaged exoplanets (*4*, *9*–*11*). Most young planets appear to be methane-free, even at temperatures where equivalent brown dwarfs show evidence of methane, suggesting nonequilibrium chemistry and persistent clouds that are probably age- and mass-dependent (*1*, *12*–*15*).

In spite of uncertainties about their atmospheric properties, the luminosities of these planets are well constrained. Luminosity is a function of age, mass, and initial conditions (*16*, *17*) and hence can provide insights into a planet's formation. Rapid formation (e.g., through global disk instabilities acting on a dynamical time scale) yields high-entropy planets that are bright at young ages ("hot start"). Alternatively, two-stage formation—in which the development of a dense solid core is followed by gas accretion through a shock, as is likely in the case of Jupiter—can produce a range of states, including lower-entropy planets that are cooler and slightly smaller in radius ("cold start"). The young directly imaged planets are almost all too bright for the cold-start model to apply, except for specific accretion shock properties; however, their formation is also difficult to explain by global instability, which should operate preferentially at higher masses and at large semimajor axis separations (*18*, *19*). In addition, these planets are close to the limit of sensitivity for first-generation large-telescope adaptive optics (AO) systems. The goal of the latest generation of surveys, which use dedicated high-contrast AO coronagraphs (*20*–*23*) such as the Gemini Planet Imager (GPI) and its counterparts, is to expand the sample of directly imaged planets to include closer separations, lower masses, and lower temperatures, a crucial empirical step toward investigating the above modes of formation.

The Gemini Planet Imager Exoplanet Survey (GPIES) is targeting 600 young nearby stars with the GPI instrument. The star 51 Eridani (51 Eri) was chosen as an early target for the survey because of its youth and proximity. Its stellar properties are given in Table 1. The star exhibits weak mid- and far-IR excess emission, indicating low-mass inner (5.5 AU) and outer (82 AU) dust belts (*24*, *25*). It also has two distant (~2000 AU) stellar companions, which constitute the 6-AU–separation M-dwarf binary system GJ 3305 (*26*). 51 Eri and GJ 3305 were classified in 2001 as members of the β Pictoris moving group (*27*), and subsequent measurements support this identification (*28*). The estimated age of the β Pictoris moving group ranges from 12 to 23 million years (My) (*27*, *29*–*32*). Giving strong weight to the group's lithium-depletion boundary age, we adopted an age of 20 ± 6 My for all four components of the 51 Eri system (*28*).

We observed 51 Eri in the H band (1.65 μm) in December 2014, as the 44th target in the GPIES campaign. GPI observations produce spectroscopic cubes with a spectral-resolving power of 45 over the entire field of view. A companion planet designated 51 Eri b, was apparent after subtraction of the point spread function (PSF). The planet is located at a projected separation of 13 AU, and its spectra exhibit distinctive strong methane and water-vapor absorption (Figs. 1 and 2). We observed 51 Eri again in January 2015 to broaden the wavelength coverage, using GPI (J band, 1.25 μm) and the W. M. Keck Observatory's Near Infrared Camera 2 (NIRC2; Lp band, 3.8 μm). The observed spectra are highly similar to those of a field brown dwarf of spectral type T4.5 to T6 (Fig. 2). The J-band spectrum confirmed methane absorption at this wavelength, and the extremely red H-Lp color is similar to that of other cool, low-mass objects (Fig. 3). The signal-to-noise ratio at J-band wavelengths is inferior to that at H-band wavelengths, and extraction introduces additional systematic effects. The J-band detection is reliable (>6σ), but the fluxes in individual spectral channels are less certain. However, the methane feature was robustly detected at both bands (*28*).

Demonstrating common proper motion (*33*), or showing that the probability of a foreground or background contaminant is extremely low, establishes the nature of directly imaged planets. The interval between the December 2014 and January 2015 observations is too brief, given our astrometric accuracy (*28*), to show that 51 Eri b and 51 Eri share proper motion and parallax. However, nondetection of 51 Eri b in archival data from 2003 (*28*) excludes a stationary background source and requires proper motion within ~0.1 arc sec/year of 51 Eri. The strong methane absorption that is evident for 51 Eri b is found only in T-type or later brown dwarfs. We determined the probability of finding a T dwarf in our field by merging the observed T-dwarf luminosity functions (*27*, *28*) and adopting the spectral types and absolute magnitudes for T dwarfs (*34*), from which we calculated a false alarm rate of 1.72×10^{-7} methane objects (i.e., types T0 to T8.5) per GPI field (>5σ). The proper motion constraint eliminates a further 66% of likely background T-dwarf proper motions. The total false alarm probability after observing 44 targets is the probability of a T-spectrum object appearing in 44 Bernoulli trials, given by the binomial distribution, which yields a final probability of 2.4×10^{-6}. Although the occurrence rate of planetary companions is not known with precision, the detection of planetary objects at similar physical separations to 51 Eri b, such as β Pic b and HR8799 e, indicates that the rate is $>10^{-3}$ per star. Hence, with the high-quality spectrum available to us, it is much more likely that 51 Eri b is a bound planetary companion than a chance alignment.

We used planetary atmosphere and evolution models to estimate the properties of 51 Eri b. We first fitted the observed J- and H-band spectra using standard cloud-free equilibrium-chemistry models, with radii constrained based on mass as given by evolutionary tracks, similar to those in (*35*). This constrained fit gives an effective temperature of 750 K, with a radius [0.76 Jupiter radius (R_J)] and surface gravity similar to those of an old (10 billion years), high-mass brown dwarf. A similar, though less extreme, result (small radii and hence high masses and old ages) is associated with several model fits to observations of the HR8799 planets (*13*, *15*, *16*), even though high

[1]Kavli Institute for Particle Astrophysics and Cosmology, Stanford University, Stanford, CA 94305, USA. [2]Lawrence Livermore National Laboratory, 7000 East Avenue, Livermore, CA 94040, USA. [3]Department of Astronomy, University of California–Berkeley, Berkeley, CA 94720, USA. [4]Lunar and Planetary Laboratory, University of Arizona, Tucson, AZ 85721, USA. [5]Center for Astrophysics and Space Sciences, University of California–San Diego, 9500 Gilman Drive, La Jolla, CA 92093, USA. [6]NASA Ames Research Center, MS 245-3, Moffett Field, CA 94035, USA. [7]National Research Council of Canada, Herzberg Institute of Astrophysics, 5071 West Saanich Road, Victoria, British Columbia V9E 2E7, Canada. [8]Department of Physics and Astronomy, University of Victoria, 3800 Finnerty Road, Victoria, British Columbia V8P 5C2, Canada. [9]Search for Extraterrestrial Intelligence Institute, Carl Sagan Center, 189 Bernardo Avenue, Mountain View, CA 94043, USA. [10]Space Telescope Science Institute, 3700 San Martin Drive, Baltimore, MD 21218, USA. [11]School of Earth and Space Exploration, Arizona State University, Post Office Box 871404, Tempe, AZ 85287, USA. [12]Institut de Recherche sur les Exoplanètes, Départment de Physique, Université de Montréal, Montréal, Québec H3C 3J7, Canada. [13]Los Alamos National Laboratory, Post Office Box 1663, MS F663, Los Alamos, NM 87545, USA. [14]Department of Physics and Astronomy, University of California–Los Angeles, 430 Portola Plaza, Los Angeles, CA 90095, USA. [15]Department of Physics and Astronomy, Centre for Planetary Science and Exploration, The University of Western Ontario, London, Ontario N6A 3K7, Canada. [16]Subaru Telescope, 650 North A'ohoku Place, Hilo, HI 96720, USA. [17]Science and Technology Research Institute, University of Hertfordshire, Hatfield AL10 9AB, UK. [18]Department of Astrophysical Sciences, Princeton University, Princeton, NJ 08544, USA. [19]Dunlap Institute for Astronomy and Astrophysics, University of Toronto, 50 St. George Street, Toronto, Ontario M5S 3H4, Canada. [20]Institut de Planétologie et d'Astrophysique de Grenoble, Université Grenoble Alpes, Centre National de la Recherche Scientifique, 38000 Grenoble, France. [21]Department of Astronomy and Astrophysics, University of Chicago, 5640 South Ellis Avenue, Chicago, IL 60637, USA. [22]Department of Astronomy and Astrophysics, University of California–Santa Cruz, Santa Cruz, CA 95064, USA. [23]Department of Physics, Durham University, Stockton Road, Durham DH1, UK. [24]Gemini Observatory, Casilla 603, La Serena, Chile. [25]Department of Physics and Astronomy, Johns Hopkins University, 3600 North Charles Street, Baltimore, MD 21218, USA. [26]University of Exeter, Astrophysics Group, Physics Building, Stocker Road, Exeter EX4 4QL, UK. [27]Department of Physics and Astronomy, University of Georgia, Athens, GA 30602, USA. [28]Large Synoptic Survey Telescope, 950 North Cherry Avenue, Tucson, AZ 85719, USA. [29]Department of Physics and Astronomy, Stony Brook University, 100 Nicolls Road, Stony Brook, NY 11794-3800, USA. [30]Department of Astronomy and Astrophysics, University of Toronto, Toronto, Ontario M5S 3H4, Canada. [31]Steward Observatory, 933 North Cherry Avenue, University of Arizona, Tucson, AZ 85721, USA. [32]Department of Physics, University of California–Santa Barbara, Broida Hall, Santa Barbara, CA 93106-9530, USA. [33]Department of Astrophysics, American Museum of Natural History, New York, NY 10024, USA. [34]Department of Engineering Science and Physics, College of Staten Island, City University of New York, Staten Island, NY 10314, USA. [35]Departamento de Astronomía, Universidad de Chile, Camino El Observatorio 1515, Casilla 36-D, Las Condes, Santiago, Chile. [36]Stratospheric Observatory for Infrared Astronomy, Universities Space Research Association, NASA Armstrong Flight Research Center, 2825 East Avenue P, Palmdale, CA 93550, USA. [37]Sibley School of Mechanical and Aerospace Engineering, Cornell University, Ithaca, NY 14853, USA. [38]Physics and Astronomy, University of Toledo, 2801 West Bancroft Street, Toledo, OH 43606, USA. [39]Jet Propulsion Laboratory, California Institute of Technology, 4800 Oak Grove Drive, Pasadena, CA 91109, USA.
***Corresponding author. E-mail: bmacintosh@stanford.edu**

Table 1. Properties of 51 Eridani and 51 Eridani b.

51 Eridani	
Spectral type	F0IV
Mass (solar masses)	1.75 ± 0.05
Luminosity ($L/L_\odot$)	7.1 ± 1
Distance (pc)	29.4 ± 0.3
Proper motion (milli-arc sec/year)	44.22 ± 0.34 (east), −64.39 ± 0.27 (north) (*44*)
Age (My)	20 ± 6
Metallicity (metal abundance over hydrogen abundance)	−0.027 (*45*)
J, H, Ks, Lp (magnitudes)	4.74 ± 0.04, 4.77 ± 0.08, 4.54 ± 0.02, 4.54 ± 0.21
Dust luminosity divided by bolometric luminosity	$\sim 10^{-6}$
51 Eri b	
Projected separation (milli-arc sec)	449 ± 7 (31 January 2015)
Projected separation (AU)	13.2 ± 0.2 (31 January 2015)
Absolute J-band magnitude	16.75 ± 0.40
Absolute H-band magnitude	16.86 ± 0.21
Absolute Lp-band magnitude	13.82 ± 0.27

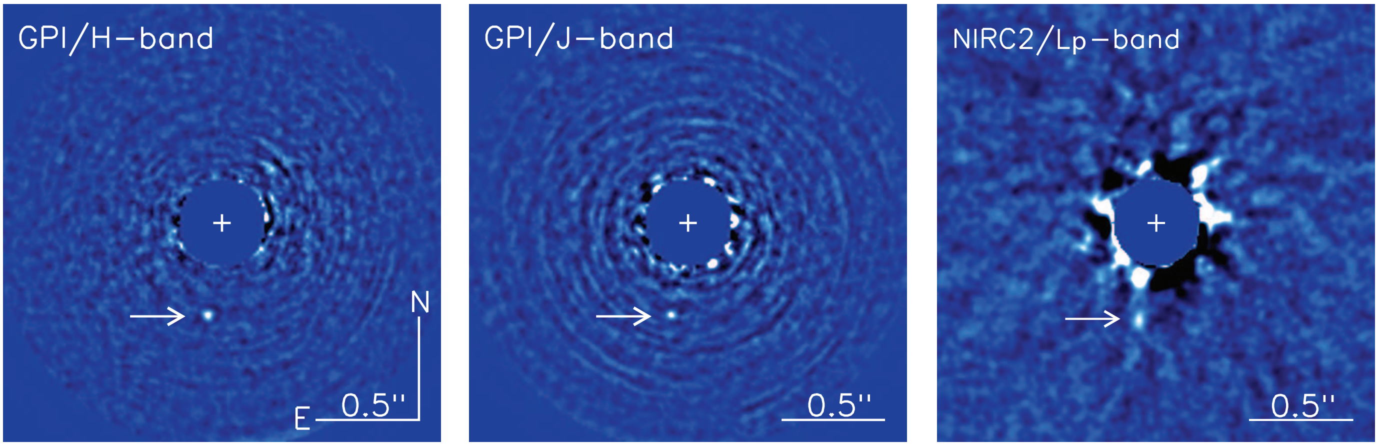

Fig. 1. Images of 51 Eri and 51 Eri b (indicated by the arrow) after PSF subtraction. (**A**) H-band GPI image from December 2014. (**B**) J-band GPI image from January 2015. (**C**) Lp-band NIRC2 image from January 2015.

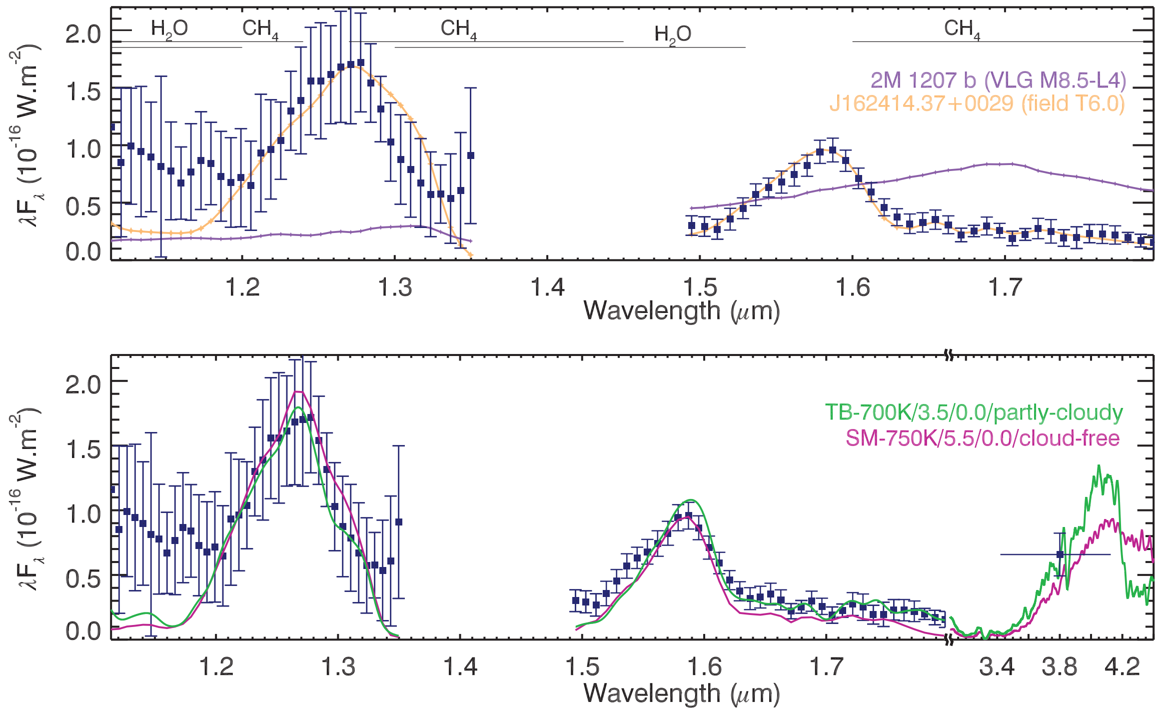

Fig. 2. J- and H-band spectra for 51 Eri b from GPI data, after PSF subtraction. Strong methane absorption, similar to that of Jupiter, is apparent. (**Top**) Spectra for the hotter young planetary object 2M 1207 b (purple) and a high–mass-field T6 brown dwarf from the SpeX library (orange) (*43*) are overplotted. (**Bottom**) Observed J and H spectra and Lp photometry with two model fits overlaid: a young, low-mass, partly cloudy object (TB-700K, green) and a higher-mass cloud-free object (SM-750K, pink). The main source of error in the extracted spectra is residual speckle artifacts, so errors in neighboring spectral channels are strongly correlated; error estimation is discussed in (*28*). λF_λ, flux.

masses are excluded by dynamical stability considerations (*36*). This model was not constrained to fit the Lp-band observation but does so within 1.6σ.

We next fitted a model to the J-H spectra and Lp photometry using a linear combination of cloudy and cloud-free surfaces and nonequilibrium chemistry, and we allowed the planet's radius to vary independently of the radii given by evolutionary tracks. Models of this type generally produce reasonable fits to other directly imaged planets (*11–13, 15, 37, 38*). This model produced a slightly lower effective temperature. The spectral shape and colors only weakly constrain gravity but favor lower masses, and the radius (~1 R_J) is consistent with evolutionary tracks, given the age of the system. Table 2 summarizes the results of the modeling. With the spectral and atmospheric uncertainties, a wide range of other models (including those with temperatures as high as ~1000 K) are also broadly consistent with the observations. The low temperature is supported by the evidence of strong methane absorption that is not observed for other planets of similar age.

The value of $\log(L/L_\odot)$, –5.4 to –5.8 (where $L/L_\odot$ is the planet's luminosity normalized by that of the Sun), is similar in all models, regardless of temperature or clouds. Combined with the age, the luminosity can be used to estimate the mass of the planet. For a hot-start model, this corresponds to a mass of ~2 $(t/20\ \mathrm{My})^{0.65}\ [(L/2\times10^{-6}\ L_\odot)^{0.54}$ M_J, the lowest-mass self-luminous planet directly imaged to date (*t*, age of the planet). 51 Eri b, unlike other young (<100 million-year-old) planetary-mass companions, has a low enough luminosity to be consistent with cold-start core-accretion scenarios. In cold-start evolution, luminosity at an age of 20 My is nearly independent of mass, so the mass of 51 Eri b would be between 2 and 12 M_J.

51 Eri b and the GJ 3305 binary system form a hierarchical triple configuration (*28*), but the companion pair is far enough away that the planet is expected to be dynamically stable in its current

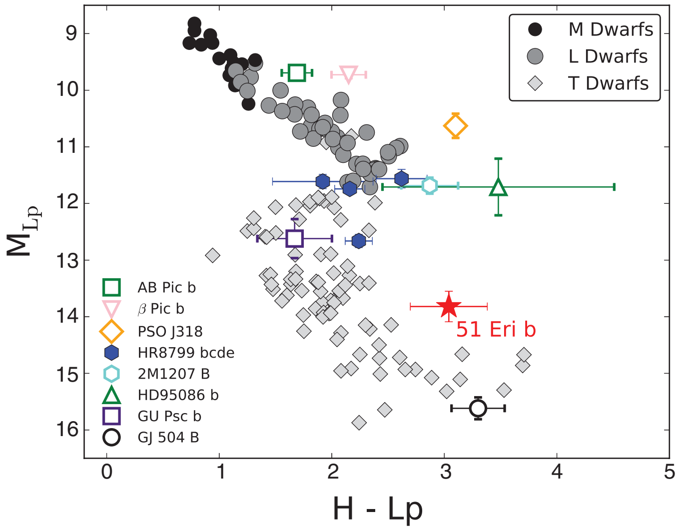

Fig. 3. Color-magnitude diagram of brown dwarfs (gray and black) and planetary-mass objects (colors). 51 Eri b is indicated with a red star, distinct from most other planets in the methane-dominated T-dwarf region of the diagram. The Lp photometry for field brown dwarfs is taken from (*45*, *46*) or converted from the Wide-field Infrared Survey Explorer W1 band (*47*) using an Lp-versus-W1 linear fit. Parallaxes are available for all objects plotted (*46*). M_{Lp}, Lp-band absolute magnitude.

Table 2. Modeling results for 51 Eri b.

	Cloud-free equilibrium model SM-750K	Partial-cloud model TB-700K
Absolute J-band magnitude	16.82	16.64
Absolute H-band magnitude	17.02	16.88
Absolute Lp-band magnitude	14.3	13.96
T_{eff} (K)	750	700
Radius (R_J)	0.76	1
Log($L/L_\odot$)	–5.8	–5.6
Log(surface gravity)	5.5	3.5
Age (My)	10,000	20 (assumed to match stellar age)
Mass (M_J)	67	2 (from luminosity, assuming a high-entropy start)

orbit (*26*). Moreover, the young age of the system suggests that although long-term dynamical effects, such as secular Lidov-Kozai oscillations, might have altered the planet's eccentricity and inclination, it is unlikely that they have had time to produce the extreme eccentricities required for tidal friction to alter the planet's semimajor axis (*39*). The formation of a ~2-M_J planet at an orbital distance of ~15 AU around a Sun-like star can be explained by modest extensions to the core-accretion theory. Early versions of the theory found that accretion of the core at larger orbital distances is in danger of taking too long, failing to capture the natal gas before it dissipates (*40*). 51 Eri b is close enough to the star that this may be less of a problem, and the addition of migration (*41*) or pebbles that experience gas drag (*42*) also helps overcome this time-scale difficulty.

The transition from L-type to T-type planets appears to occur over a narrow range of temperatures, between ~1000 K (HR8799 b and PSO J318.5-22) (*42*) and 700 K (51 Eri b). Direct determination of an object's mass, either through spectral surface gravity indicators or reflex astrometry of the primary star, could determine whether it formed through hot- or cold-start processes. 51 Eri b provides an opportunity to study in detail a planet that is still influenced by the initial conditions of its formation. With a methane-dominated spectrum, low luminosity, and a potentially low-entropy start, 51 Eri b is a bridge between wider-orbit, hotter, more massive planets and planets at Jupiter-like scales.

REFERENCES AND NOTES

1. C. Marois *et al.*, *Science* **322**, 1348–1352 (2008).
2. P. Kalas *et al.*, *Science* **322**, 1345–1348 (2008).
3. A.-M. Lagrange *et al.*, *Science* **329**, 57–59 (2010).
4. M. Kuzuhara *et al.*, *Astrophys. J.* **774**, 11 (2013).
5. J. C. Carson *et al.*, *Astrophys. J.* **763**, L32 (2013).
6. J. Rameau *et al.*, *Astrophys. J.* **772**, L15 (2013).
7. V. Bailey *et al.*, *Astrophys. J.* **780**, L4 (2014).
8. D. Lafrenière, R. Jayawardhana, M. H. van Kerkwijk, *Astrophys. J.* **689**, L153–L156 (2008).
9. M. Janson *et al.*, *Astrophys. J.* **778**, L4 (2013).
10. M.-E. Naud *et al.*, *Astrophys. J.* **787**, 5 (2014).
11. T. S. Barman, Q. M. Konopacky, B. Macintosh, C. Marois, Simultaneous detection of water, methane and carbon monoxide in the atmosphere of exoplanet HR8799b, http://xxx.lanl.gov/abs/1503.03539.
12. T. S. Barman, B. Macintosh, Q. M. Konopacky, C. Marois, *Astrophys. J.* **733**, 65 (2011).
13. A. J. Skemer *et al.*, *Astrophys. J.* **792**, 17 (2014).
14. M. S. Marley *et al.*, *Astrophys. J.* **754**, 135 (2012).
15. N. Madhusudhan, A. Burrows, T. Currie, *Astrophys. J.* **737**, 34 (2011).
16. M. S. Marley, J. J. Fortney, O. Hubickyj, P. Bodenheimer, J. J. Lissauer, *Astrophys. J.* **655**, 541–549 (2007).
17. D. S. Spiegel, A. Burrows, *Astrophys. J.* **745**, 174 (2012).
18. R. R. Rafikov, *Astrophys. J.* **648**, 666–682 (2006).
19. K. M. Kratter, R. Murray-Clay, A. N. Youdin, *Astrophys. J.* **710**, 1375–1386 (2010).
20. J.-L. Beuzit *et al.*, SPHERE Consortium, paper presented at In the Spirit of Lyot 2010: Direct Detection of Exoplanets and Circumstellar Disks, Paris, 25 to 29 October 2010; abstract available at http://adsabs.harvard.edu/abs/2010lyot.confE.44B.
21. N. Jovanovic *et al.*, The Subaru Coronagraphic Extreme Adaptive Optics system: Enabling high-contrast imaging on solar-system scales, http://xxx.lanl.gov/abs/1507.00017.
22. B. R. Oppenheimer *et al.*, *Proc. SPIE* **8447**, 844720 (2012).
23. B. Macintosh *et al.*, *Proc. Natl. Acad. Sci. U.S.A.* **111**, 12661–12666 (2014).
24. R. I. Patel, S. A. Metchev, A. Heinze, *Astrophys. J. Suppl. Ser.* **212**, 10 (2014).
25. P. Riviere-Marichalar *et al.*, *Astron. Astrophys.* **565**, A68 (2014).
26. M. Janson *et al.*, *Astrophys. J. Suppl. Ser.* **214**, 17 (2014).
27. B. Zuckerman, I. Song, M. S. Bessell, R. A. Webb, *Astrophys. J.* **562**, L87–L90 (2001).
28. Material and methods are available as supplementary materials on *Science* Online.
29. M. Simon, G. H. Schaefer, *Astrophys. J.* **743**, 158 (2011).
30. A. S. Binks, R. D. Jeffries, *Mon. Not. R. Astron. Soc. Lett.* **438**, L11–L15 (2014).
31. E. E. Mamajek, C. P. M. Bell, *Mon. Not. R. Astron. Soc.* **445**, 2169–2180 (2014).
32. T. D. Brandt *et al.*, *Astrophys. J.* **786**, 1 (2014).
33. G. Chauvin *et al.*, *Astron. Astrophys.* **438**, L25–L28 (2005).
34. J. D. Kirkpatrick, *et al.*, *Astrophys. J.* **753**, 156 (2012).
35. D. Saumon, M. S. Marley, *Astrophys. J.* **689**, 1327–1344 (2008).
36. D. C. Fabrycky, R. A. Murray-Clay, *Astrophys. J.* **710**, 1408–1421 (2010).
37. J. Chilcote *et al.*, *Astrophys. J.* **798**, L3 (2015).
38. T. Currie *et al.*, *Astrophys. J.* **795**, 133 (2014).
39. D. Fabrycky, S. Tremaine, *Astrophys. J.* **669**, 1298–1315 (2007).
40. J. B. Pollack *et al.*, *Icarus* **124**, 62–85 (1996).
41. Y. Alibert, C. Mordasini, W. Benz, C. Winisdoerffer, *Astron. Astrophys.* **434**, 343–353 (2005).
42. M. Lambrechts, A. Johansen, *Astron. Astrophys.* **544**, A32 (2012).
43. This research has benefitted from the SpeX Prism Spectral Libraries, maintained by A. Burgasser at http://pono.ucsd.edu/~adam/browndwarfs/spexprism.
44. F. van Leeuwen, *Astron. Astrophys.* **474**, 653–664 (2007).
45. E. R. Houdebine, C. J. Butler, D. Garcia-Alvarez, J. Telting, *Mon. Not. R. Astron. Soc.* **426**, 1591–1605 (2012).
46. B. A. Macintosh *et al.*, *Proc. SPIE* **7015**, 701518 (2008).
47. J. K. Chilcote *et al.*, *Proc. SPIE* **8446**, 84468W (2012).

ACKNOWLEDGMENTS

This work is based on observations obtained at the Gemini Observatory, which is operated by the Association of Universities for Research in Astronomy under a cooperative agreement with NSF on behalf of the Gemini partnership, whose membership includes: NSF (United States); the National Research Council (Canada); the Comisión Nacional de Investigación Científica y Tecnológica (Chile); the Australian Research Council (Australia); the Ministério da Ciência, Tecnologia e Inovação (Brazil); and Ministerio de Ciencia, Tecnología e Innovación Productiva (Argentina). The research was supported by grants from NSF, including AST-1411868 (B.M., K.F., J.P., and A.R.), AST-0909188 and AST-1313718 (J.R.G., P.K., R.D.R., and J.W.), AST-1413718 (M.P.F. and G.D.), and AST-1405505 (T.B.). Support was also provided by grants from NASA, including NNX14AJ80G (B.M., F.M., E.N., and M.P.), NNH15AZ591 (D.S. and M.M.), NNX15AD95G (J.R.G. and P.K.), NNX11AD21G (J.R.G. and P.K.), and NNH11ZDA001N (S.M. and R.P.). J.R., R.D., and D.L. acknowledge support from the Fonds de Recherche du Quebec. Support is acknowledged from NSF fellowships DGE-123825 (A.Z.G.), DGE-1311230 (K.W.-D.), DGE-1232825 (S.G.W.), and DGE-1144087 (L.W.H.). Portions of this work were performed under the auspices of the U.S. Department of Energy by Lawrence Livermore National Laboratory under contract DE-AC52-07NA27344. GPI data are archived at the Gemini Science Archive: www.cadc-ccda.hia-iha.nrc-cnrc.gc.ca/en/gsa/.

SUPPLEMENTARY MATERIALS

www.sciencemag.org/content/350/6256/64/suppl/DC1
Materials and Methods
Figs. S1 to S3
Tables S1 to S3
References (*48*–*90*)

17 May 2015; accepted 3 August 2015
Published online 13 August 2015
10.1126/science.aac5891

Discovery and spectroscopy of the young jovian planet 51 Eri b with the Gemini Planet Imager

B. Macintosh, J. R. Graham, T. Barman, R. J. De Rosa, Q. Konopacky, M. S. Marley, C. Marois, E. L. Nielsen, L. Pueyo, A. Rajan, J. Rameau, D. Saumon, J. J. Wang, J. Patience, M. Ammons, P. Arriaga, E. Artigau, S. Beckwith, J. Brewster, S. Bruzzone, J. Bulger, B. Burningham, A. S. Burrows, C. Chen, E. Chiang, J. K. Chilcote, R. I. Dawson, R. Dong, R. Doyon, Z. H. Draper, G. Duchêne, T. M. Esposito, D. Fabrycky, M. P. Fitzgerald, K. B. Follette, J. J. Fortney, B. Gerard, S. Goodsell, A. Z. Greenbaum, P. Hibon, S. Hinkley, T. H. Cotten, L.-W. Hung, P. Ingraham, M. Johnson-Groh, P. Kalas, D. Lafreniere, J. E. Larkin, J. Lee, M. Line, D. Long, J. Maire, F. Marchis, B. C. Matthews, C. E. Max, S. Metchev, M. A. Millar-Blanchaer, T. Mittal, C. V. Morley, K. M. Morzinski, R. Murray-Clay, R. Oppenheimer, D. W. Palmer, R. Patel, M. D. Perrin, L. A. Poyneer, R. R. Rafikov, F. T. Rantakyrö, E. L. Rice, P. Rojo, A. R. Rudy, J.-B. Ruffio, M. T. Ruiz, N. Sadakuni, L. Saddlemyer, M. Salama, D. Savransky, A. C. Schneider, A. Sivaramakrishnan, I. Song, R. Soummer, S. Thomas, G. Vasisht, J. K. Wallace, K. Ward-Duong, S. J. Wiktorowicz, S. G. Wolff, and B. Zuckerman

Science **350** (6256), . DOI: 10.1126/science.aac5891

An exoplanet extracted from the bright

Direct imaging of Jupiter-like exoplanets around young stars provides a glimpse into how our solar system formed. The brightness of young stars requires the use of next-generation devices such as the Gemini Planet Imager (GPI). Using the GPI, Macintosh *et al.* discovered a Jupiter-like planet orbiting a young star, 51 Eridani (see the Perspective by Mawet). The planet, 51 Eri b, has a methane signature and is probably the smallest exoplanet that has been directly imaged. These findings open the door to understanding solar system origins and herald the dawn of a new era in next-generation planetary imaging.

Science, this issue p. 64; see also p. 39

Science (ISSN 1095-9203) is published by the American Association for the Advancement of Science. 1200 New York Avenue NW, Washington, DC 20005. The title *Science* is a registered trademark of AAAS.